ELECTRONICS COOLING FOR PHENIX MVD

I. INTRODUCTION

Initial calculational results have been reported for the original design of the Phenix Multiplicity and Vertex Detector (MVD)[1]. To maintain the MVD at optimized operational status, the maximum temperature of the Multi-Chip Modules(MCM) must be below 40^{0}C. To meet this requirement, the configuration of the plenum chamber, the power dissipated by the silicon chips, and airflow velocity must be examined.

The structure of the MVD has been described earlier and it was also mentioned that any two MVD plenum chambers are identical and are made of 12 parallepipedic Rohacell modules. The configuration of these two plenum chambers has been updated in the latest design. The fully populated modules (first and second module of each end) contain 6 MCM plates with 3 different spacings, while all other modules contain 4 MCMs as shown in Fig. 1. The distance between the first MCM and the shell on either side is about 4 mm. Groves 2 mm deep are cut into the upper and lower sides of the Rohacell to maintain the MCMs in place.

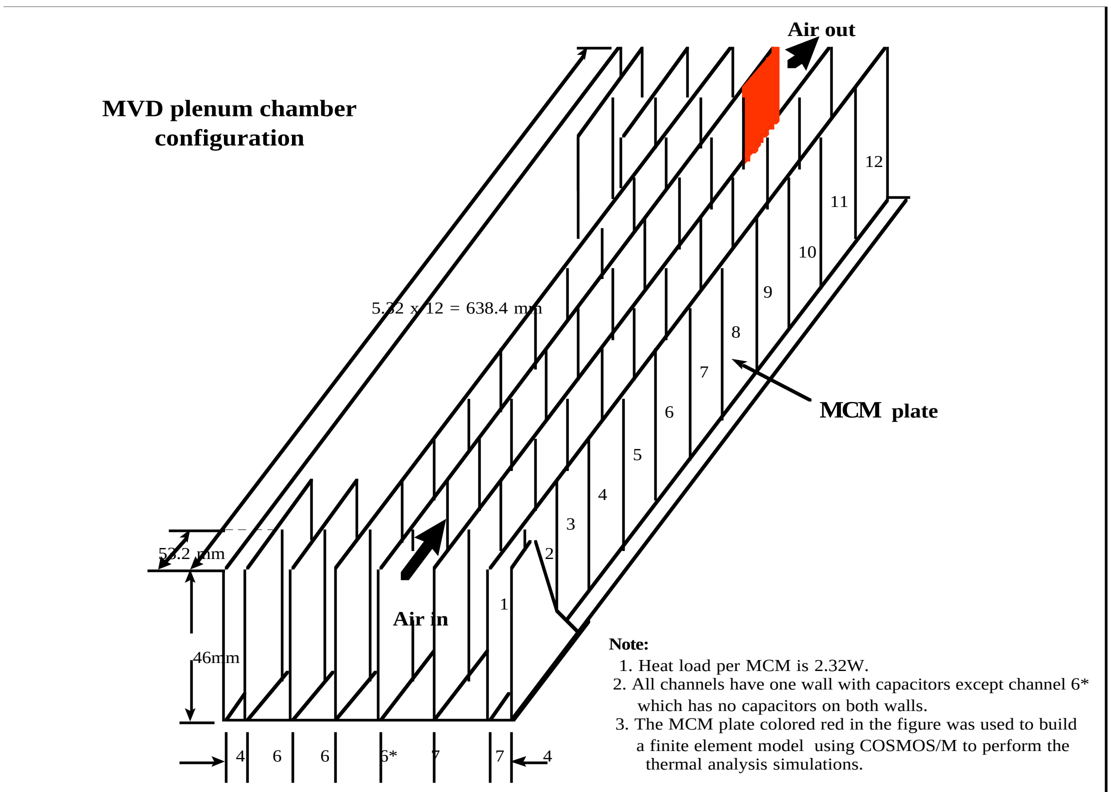

Fig. 1: MVD plenum chamber configuration

The MCMs are the main heat source in the system and each one dissipates about 2.32 W which is less than the MCM power used for the earlier analysis. The updated MCM parameters are shown in Fig. 2. This figure shows that the location of the chips, chip size, and substrate material are also different from the earlier analysis. The electronics boards are thermally isolated from the rest of the MVD by the foam shell and therefore become the only components that need to be cooled. The thermal requirement for the electronics components is to maintain the operational temperature below 50^0C. However, the temperature of the MCM's must be below 40^0C to provide an adequate safety margin. Air cooling for the design was used.

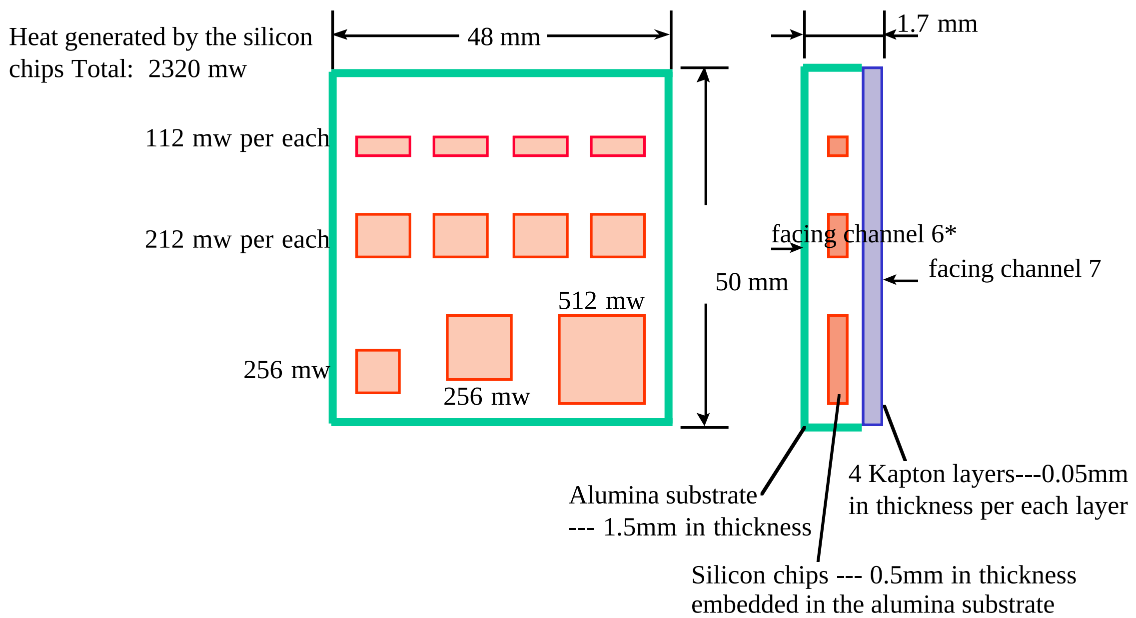

Fig. 2 MCM Parameters

II. SOLUTION PROCEDURE

1. HEATING OF AIR ALONG A CHANNEL IN THE FLOW DIRECTION

As shown in Fig. 1, inside one MVD plenum chamber, each two consecutive rows of MCMs provide an individual channel for air to flow. Only the worst case, according to the spacing of these channels and heat generated by the MCMs, will be picked to study the heat transfer phenomena.

Assuming that the temperature is uniform across the channel cross section, the air temperature at some distance d from the inlet, T_{air}, is equal to the air temperature at the inlet, T_{inlet}, plus a temperature increase corresponding to the heating of the air through the channel. Thus the air temperature is given by

$$T_{air} = T_{inlet} + Q/\rho \ v \ A_c \ C_p \ , \qquad (1)$$

where Q is the total heat load from the inlet to d, assuming a uniform heat load distribution along the channel. The other variables in Eq. (1) are defined as

$Q = (2.32 \text{ w}) (12)(d/L)$,

L = total length of the channel = 53.2mm x 12=0.6384 m,
d = distance along the channel =53.2mm x MCM number,
ρ = the air density at room temperature (20^0C) = 1.057219 kg/m^3,
C_p = the air specific heat at 20^0C = 1004.579 W s/kg K,
v = the airflow velocity that needs to be determined in this study, and
A_c= the channel cross section.

Between two fully populated rows of MCMs the cross section area is the one parameter that determines the velocity of the chilled air. In the current design there are four sizes of spacing. At first, we assume an air velocity for the channel flow. The worst case is where the air will be heated more than in the other channels. Using equation (1) and any assumed airflow velocity, it can be determined that the channel with the mark 6* is the channel that we should use for the heat transfer evaluation since the combination of the cross section area and heat load will give the highest temperature in the MCM. In Fig. 3 the air temperature is shown along the channels in the flow direction for four different spacing, a velocity of 9m/s, and a 20^0C inlet temperature. The outlet air temperature corresponds to the air temperature at the 12^{th} module.

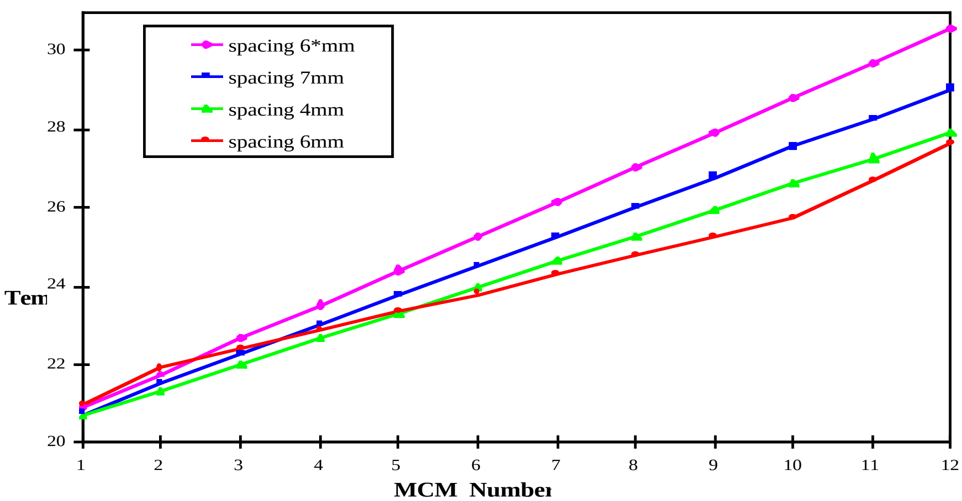

Fig. 3 Air temperature along the channel with different spacings

Thus, Fig. 3 shows that for any air flow velocity channel 6* will always give the highest outlet temperature.

2. MCM-TO-AIR THERMAL EXCHANGE

The average temperature of the MCM, T_{MCM}, is equal to the air flow temperature, T_{air}, plus a temperature differential from the exchange process between the air and the MCM plate. Thus, the average temperature reached by the MCM is

$$T_{MCM} = T_{air} + Q_{MCM} / h\, A_{MCM} \qquad (2)$$

where Q_{MCM} is the heat load dissipated by one side of the MCM and is assumed to be half of the heat load per MCM in the current design. The value of the variable in Eq (2) are

Q_{MCM} = 1.16 W,
A_{MCM} = the MCM surface area exposed to air flow = 2.4472×10^{-3} m^2, and
h = the heat transfer coefficient that depends on the flow regime (laminar or turbulent).
For a laminar flow, this coefficient is given by Sieder and Tate [2] as

$$h = 1.86\,(k/D_h)\,(Re\,Pr\,D_h/L)^{0.33}. \qquad (3)$$

For a fully developed turbulent flow, Dittus and Boelter [3] have given the following relation for h as

$$h = 0.023\,(k/D_h)\,(Re)^{0.8}(Pr)^{0.4}. \qquad (4)$$

In equations (3) and (4),
k = the air thermal conductivity at 20^0C = 2.5435×10^{-2} (W/m K),
D_h = hydraulic diameter = 1.0615×10^{-2} (m^2) for the channel with spacing 6*mm,
= 1.2151×10^{-2} (m^2) for the channel with spacing 7mm, and
Pr = the Prandtl number at room temperature = 0.72.
The Reynolds number is given by the equation

$$Re = v\,D_h/\nu, \qquad (5)$$

where ν = the air kinematic viscosity at the room temperature (20^0C)= 1.52×10^{-5} m^2/s
The airflow character depends on the value of Reynolds number. For a laminar flow, Re is less than 2000, otherwise, the flow is turbulent. As shown in Fig. 4, channel 6*, near the inlet, the thermal boundary layer is not fully developed flow. To change the flow condition, the velocity has to be changed and the average temperature reached by the MCM plate depends on airflow velocity. From Fig. 4 it shows that if we use a velocity of 9m/s, the average temperature reached by the MCM plate will be lower than the cooling requirement of 40^0C.

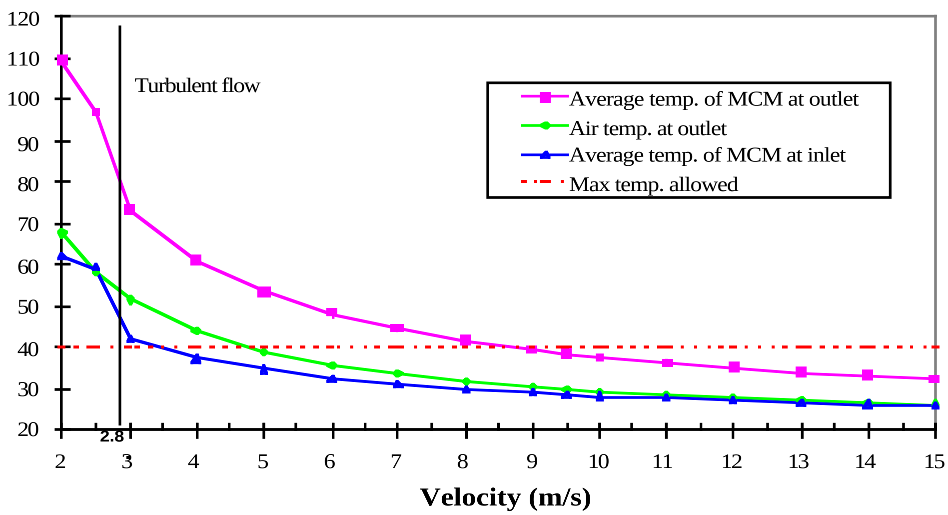

Fig. 4: Average temperature reached by the MCMs located at the inlet and the outlet versus the airflow velocity in the channel within spacing 6* mm

To verify that the velocity of 9m/s is the appropriate selection for this design, a calculation for the temperature reached by the MCM plates along the channel 6* has been completed and these temperatures are plotted in Fig. 5 for several airflow velocities.

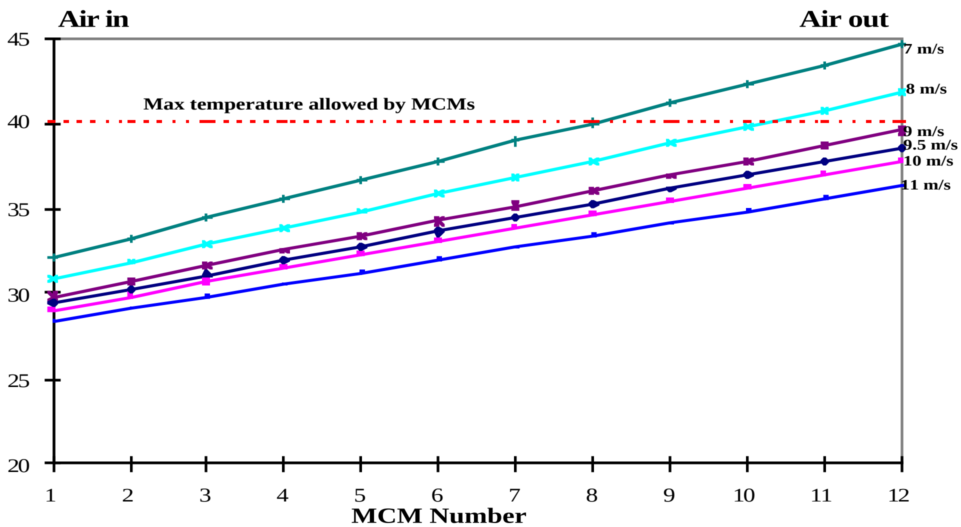

Fig. 5: Average Temperature reached by the MCMs for the 12 modules while air flow through channel 6* for several airflow velocities

As shown in Fig. 5, at any given airflow velocity, the average temperature reached by the MCM plates is a function of the air temperature along the channel. The temperature differential for the MCM-to-air thermal exchange is constant as given by Q_{MCM} / h A_{MCM}. Therefore, for a given airflow velocity, the MCM temperature is a linear function of the distance from the inlet. The MCM plate that is located at the outlet is the least cooled since the air temperature is the warmest there. In Fig. 4 and Fig. 5, it is shown that the airflow velocity needed to maintain all MCMs below 40^0C is at least 9m/s.

The airflow velocity of 9m/s in the channel 6* produces an average heat transfer coefficient of 52.72 W/m^2 ^{0}C and the outlet air temperature in this channel will reach 30.55^0C. To determine the MCM plate which is cooled least and therefore represents the maximum temperature reached at a MVD, an evaluation has also been done for a channel spacing of 7mm. In Fig. 3 the second highest outlet air temperature is for a channel with a spacing of 7mm. With an airflow velocity of 9m/s, an average heat transfer coefficient of 51.32 W/m^2 ^{0}C is produced in this channel and the outlet air temperature is 29.05^0C. The MCM plate that is located at the outlet of the plenum chamber and between channels with a spacing 6*mm and 7mm is shown in Fig. 1 as the MCM plate with red color.

The spreadsheets used for the above calculations are attached in Appendix 1, 2 and 3.

3. MCM HEAT SPREADING

All parameters of a MCM are shown in Fig. 2. It is made of alumina as a substrate material with 1.5mm in thickness; silicon chips embedded in alumina substrate 0.5mm deep; and kapton covers with four very thin layers (0.05mmx4) as shown in Fig. 2.

The silicon chips have 5 different sizes and dissipate more or less heat as shown in the front view of Fig. 2. The chips that are located in the first and second rows dissipate 0.112 W and 0.212 W each, respectively. In the third row there are two silicon chips dissipate 0.256 W each. The third chip dissipates the largest heat of 0.512 W.

Using COSMOS/M HSTAR for the heat transfer analysis, a finite element model of a typical MCM plate (the one with the red color as shown in Fig. 1) was created to simulate a 9m/s airflow and convective heat transfer on both sides of this plate. As described in section 2 of the solution procedure, one side of this MCM plate faces channel 6*, where the ambient air temperature was set to a computed outlet air temperature of 30.55^0C. The average heat transfer coefficient was set to 52.72 W/m^2 ^{0}C, which corresponds to a 9m/s airflow for this channel. On the other side of this MCM plate is channel 7, and from the computed results, the ambient air temperature was set to 29.05^0C. The average heat transfer coefficient was set to 51.32 W/m^2 ^{0}C.

In addition to the ambient air temperature and the average heat transfer coefficients, the boundary conditions for this model also include the volumetric energy dissipated from the chips. They are:

- in the first row, the volumetric energy dissipated by the chips: 8.696×10^{-3} W/mm^3
- in the second row, the volumetric energy dissipated by the chips: 7.681×10^{-3} W/mm^3
- in the third row, the volumetric energy dissipated by the left chip: 1.422×10^{-2} W/mm^3
- in the third row , the volumetric energy dissipated by the central chip: 5.331×10^{-3} W/mm^3
- in the third row , the volumetric energy dissipated by the right chip: 6.300×10^{-3} W/mm^3

The finite element analysis was performed for a model which contains 3 layers of material with different

thermal conductivities as shown in Fig. 6. The first layer facing channel 6* is pure alumina substrate, 1.0mm in thickness with a thermal conductivity of 29.427×10^{-3} W/mm K. The second layer, middle one, is 0.5 mm in thickness, contains alumina substrate, and all silicon chips have a thermal conductivity of 148×10^{-3} W/mm K. The third layer facing the channel with 7mm spacing is the kapton cover which is made of four mini layers and the total thickness is 0.2mm with a thermal conductivity of 0.2×10^{-3} W/mm K.

The thermal analysis for the MCM plate was carried out to determine the temperature distribution and heat flux contours which will identify hot spot locations. The MCM model built using COSMOS/M is shown in Fig. 6. This figure also indicates the locations where the temperature distribution and heat flux contours are plotted in Fig. 7 and 8.

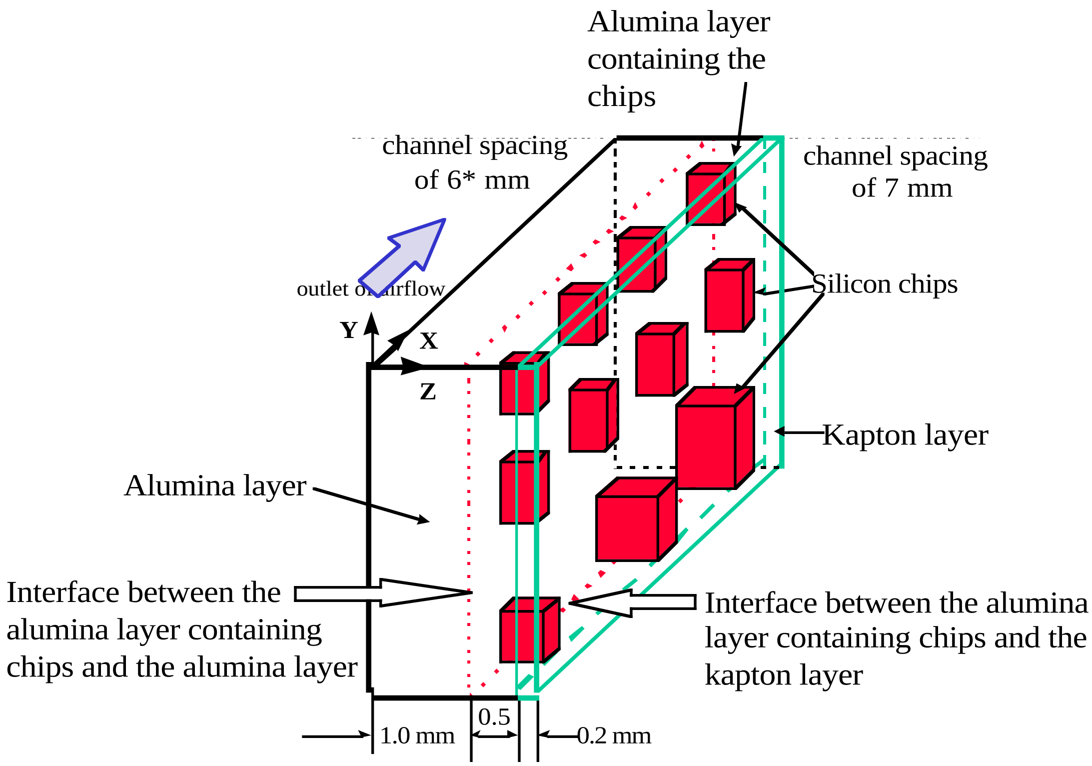

Fig. 6: MCM structural sketch

The temperature contours of the kapton surface and the alumina surface are shown in Fig. 7(a) and (b), respectively. To find the hottest spots in the electronic system for the MVD, the nodes that are the hot spots and represent the maximum temperature on the MCM plate have to be found. Therefore, the temperature contours on both sides of the alumina containing the silicon chips are plotted and are shown in Fig. 7 (c) and (d). The average temperature on the MCM plate is 312.1^{0}K (39.1^{0}C), which agrees well with the 38.9^{0}C calculated by hand as shown in Appendix 2 and 3. The maximum temperature on the MCM plate which is represented by the hot spots is 313.7^{0}K (40.7^{0}C) that is 0.7^{0}C higher than the maximum temperature reached by the MCM in the design requirement and it is 1.6^{0}C higher than the average maximum temperature reached by the MCM. The total temperature difference across the entire plate is 3.2^{0}C. The maximum hot spot is located in the central part of the biggest chip. This is not surprising since the high volumetric energy is dissipated into a big volume that is closely surrounded by additional energy dissipaters. The smaller chip in the third row left which dissipates the highest volumetric energy, has no hot spot and is cooler than the right one. This is because this chip is not close to the other chips and its small volume allows the heat to be dissipated easily to the environment.

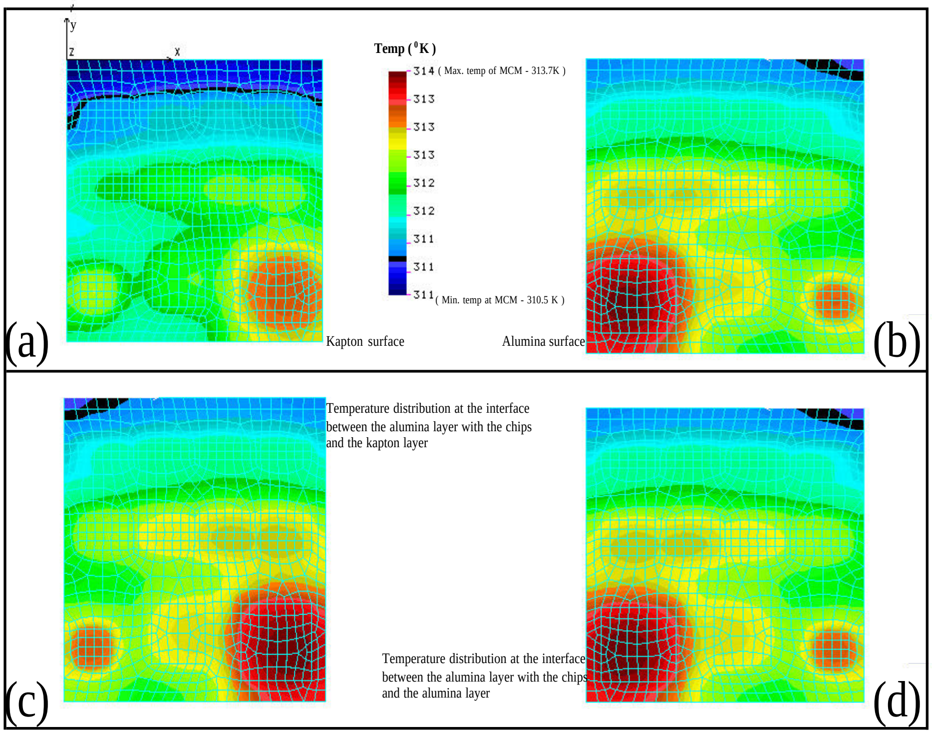

Fig. 7: Temperature distribution for the current design. Contour (a) is for the kapton surface; Contour (b) shows the Alumina surface; Contour (c) is located at the interface of alumina layer containing the chips and the kapton layer; Contour (d) is located at the interface of alumina layer containing the chips and the pure alumina layer.

Heat flux contours are shown in Fig. 8 and describe the magnitude and direction of the heat flux. On the legend, the positive heat flux is the heat flux to the kapton surface and the negative heat flux is to the alumina surface. The heat flux distribution is similar to the temperature distribution since the value of the heat flux is equal to the temperature difference between the air and the MCM plate multiplied by the average thermal coefficient which depends on the thermal conductivity of the material. This explains why the heat flux is larger toward the alumina than to the kapton. Fig. 8 (a) shows the heat flux contour on the kapton surface where the area in dark red (HF about 5.7×10^{-4} W/mm^2) indicates where the temperature is higher and the hot spots are located. But on the alumina surface as shown in Fig. 8 (b), the higher heat flux (about 10×10^{-4} -18.5×10^{-4} W/mm^2)is blue and dark blue in color and are in the higher temperature area. The yellow color area is where little heat is dissipated by the silicon chips and the lower heat flux results in a lower temperature.

s

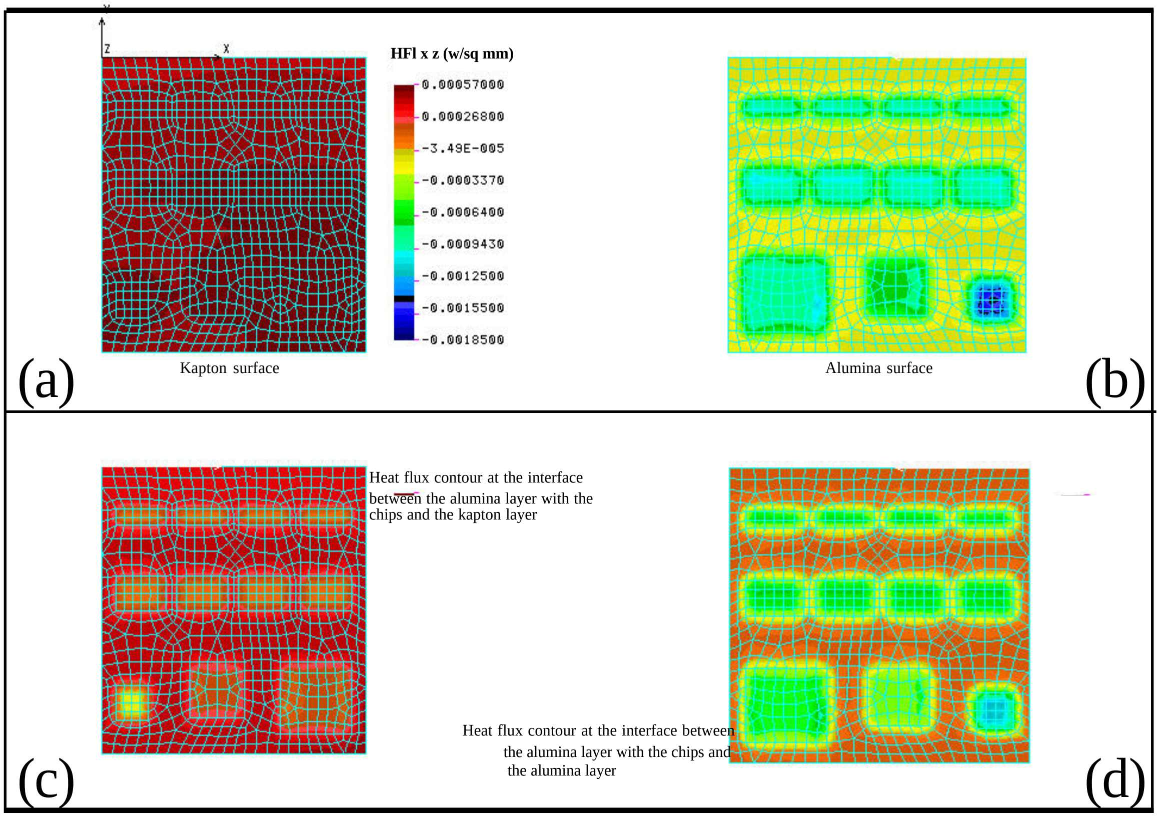

Fig. 8: **Heat flux contours for the current design. Contour (a) is for the kapton surface. Contour (b) shows the heat flux on the alumina surface. Contour (c) is located at the interface of the alumina layer containing the chips and kapton layer. Contour (d) is located at the interface of the alumina layer containing the chips and alumina layer.**

Fig. 9 shows a summary of the heat transfer phenomena for the MCM plate.

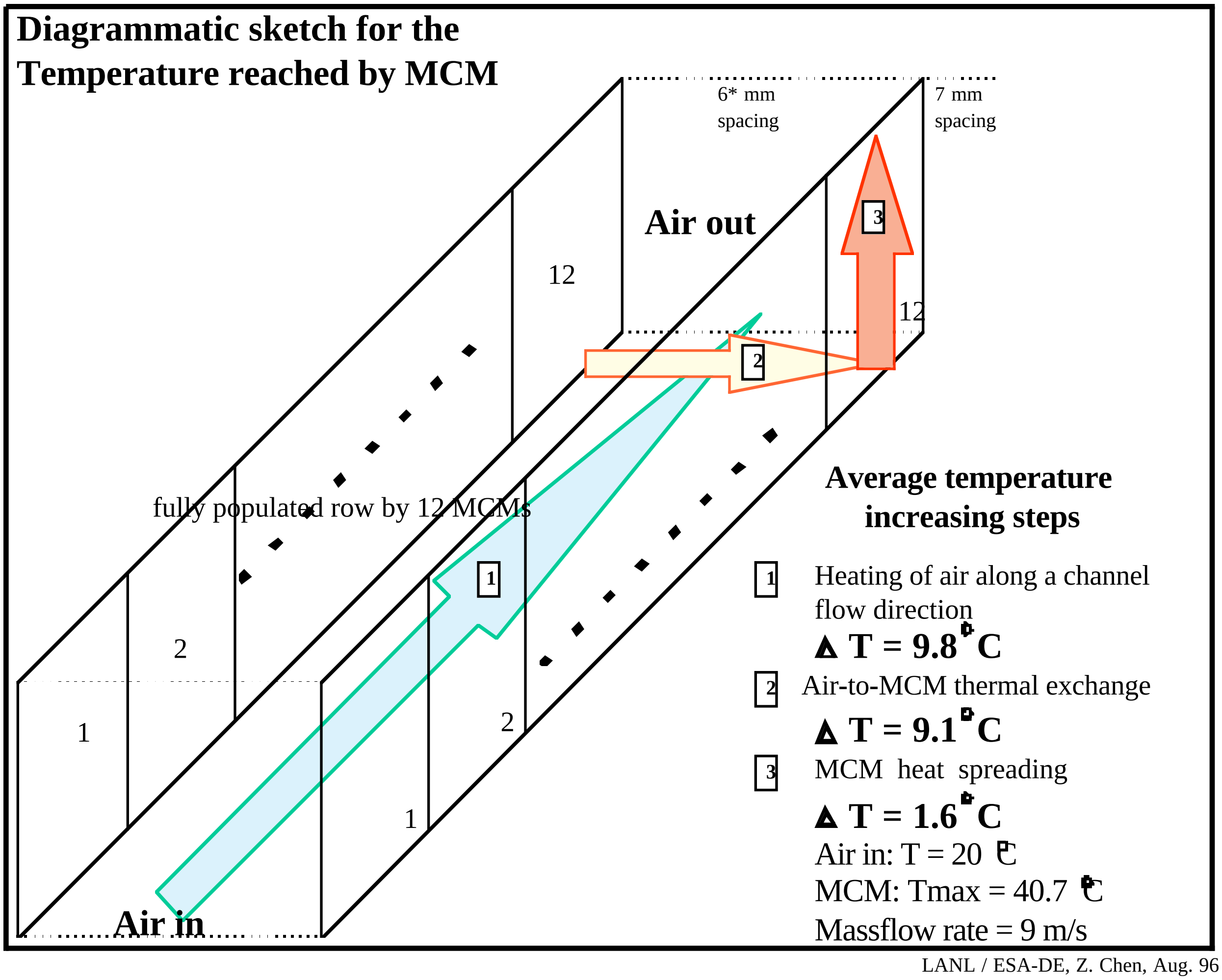

Fig. 9: Diagrammatic sketch for the Temperature reached by the MCM

III. SUMMARY

The new MCM design has been analyzed for cooling effectiveness. For the current MCM design, using an air cooling system with 9m/s airflow velocity, the average maximum temperature reached by the MCMs is 39.1^0C. The maximum temperature which is represented by the hot spots on the MCM is 40.7^0C which is a little higher than the design temperature requirement.

For the MCM design, the most important parameter is the system heat load that dominates the results

from all three phenomena. The thermal transfer coefficient is another major parameter to determine the thermal exchange of air -to-MCM and heat spreading on the MCM plate. Actually, the thermal coefficient depends on the conductivity of the MCM material and is related to the airflow Reynolds number which depends on the configuration of the airflow channel.

To avoid any failures by temperature over the design requirement, using cooler inlet air directly lowers the maximum temperature reached by the MCM. Also increasing the airflow from 9 m/s to 9.5 m/s will lower the maximum temperature of the same MCM by approximately 1^0C. The detailed calculational results is in Appendix 1.

REFERENCES

[1] Parietti, L., Potter, C., Thompson, T., Martin, D., "ESA-DE PHENIX MVD DESIGN REVIEW" a progress report, January 1996.
[2] Seider, F. and Tate, G., ind. Eng. Chem., 28, 1429 (1936).
[3] Dittus, F. and Boelter, L., University of California, Publ. Eng., 2, 443 (1930)

ZC

cy: w/att

B. Jacak, P-25, MS H846

J. Boissevain, P-25, MS H846

J. Kapustinsky, P-25, MS H846

J. Simon-Gillo, P-25, MS H846

R. Martin, ESA-DE, MS H821

W. Gregory, ESA-DE, MS H821

Z. Chen, ESA-DE, MS H821

w/o att.

T. Thompson, ESA-DE, MS H821

J. Erickson, ESA-DE, MS H821

ESA-DE File